J. Fluid Mech. (1991), *vol.* 226, *pp.* 349–369
Printed in Great Britain

Convection and particle entrainment driven by differential sedimentation

By HERBERT E. HUPPERT[1], ROSS C. KERR[2], JOHN R. LISTER[2]† AND J. STEWART TURNER[2]

[1] Institute of Theoretical Geophysics, Department of Applied Mathematics and Theoretical Physics, University of Cambridge, Silver Street, Cambridge CB3 9EW, UK

[2] Research School of Earth Sciences, Australian National University, GPO Box 4, Canberra 2601, ACT, Australia

(Received 19 June 1990)

When a suspension of small particles is overlain by a clear fluid whose density is greater than that of the interstitial fluid, but less than that of the bulk suspension, the settling of the dense suspended particles can lead to vigorous convection in the overlying fluid. This novel situation is investigated experimentally and theoretically. A sharp interface is observed between the convecting upper region and a stagnant lower region in which there is unimpeded sedimentation at low Reynolds number. There is no transport of fluid from the upper region into the lower, though there is mixing of both buoyant fluid and entrained particles from the lower region into the upper. The interface between the two regions is found to descend at a constant velocity. Systematic laboratory measurements have determined how this velocity depends on the densities of the layers and the distributions of settling velocities of the particles. A theoretical description is developed which calculates the evolution of the density of the lower region due to differential sedimentation of polydisperse particles. Buoyancy arguments based on the calculated density profile are used to place upper and lower bounds on the amount of particle entrainment into the upper layer and on the rate of fall of the interface between the convecting and sedimenting regions. The theoretical predictions are in good agreement with the experimental observations. The analysis of the interaction between convection and sedimentation in the system considered here may be particularly relevant to the description of evolving crystal-rich layers in magma chambers and of silt-laden outflow from rivers, and has a wide range of other industrial, environmental and geological applications.

1. Introduction

The fluid dynamics of convecting, particulate suspensions is of great relevance to chemical and civil engineers, geologists, metallurgists and oceanographers. Diverse applications include the transport of soil, silt and sand in rivers and estuaries, volcanic flows of suspensions of hot air and ash, the evolution of bodies of magma rich in crystals and the cooling and solidification of molten alloys containing suspended crystals and impurities. Most studies are based totally on the equations of low-Reynolds-number hydrodynamics because of the small size of the particles, as reviewed by Davis & Acrivos (1985). In this paper we will describe laboratory experiments and a related theoretical description in which, while some of the small

† Present address: Institute of Theoretical Geophysics, Department of Applied Mathematics and Theoretical Physics, University of Cambridge, Silver Street, Cambridge CB3 9EW, UK.

particles sediment in the usual way, others are transported in released, relatively light fluid that undergoes vigorous convective motions.

Consider a well-mixed suspension of heavy particles, for which the bulk density of the suspension will exceed that of the interstitial fluid. For a simple suspension of particles of uniform size and density the behaviour is well understood: the particles sediment at a rate which is dependent on their initial concentration and clear fluid is left behind a relatively sharp interface. Our interest lies in the novel situation which arises when a suspension is overlain by a fluid whose density ρ_U is intermediate between that of the bulk suspension ρ_B and that of the interstitial fluid ρ_I. Although the initial bulk-density gradient is statically stable, the settling of the dense particles in the lower layer leaves behind light interstitial fluid. This fluid convects into the upper layer and carries with it some of the particles. As a result of the entrainment of particles into the upper layer, the interface at the top of the sedimenting region can fall much more rapidly than if there were no overlying fluid. For the case of a polydisperse suspension, the differential sedimentation of the particles creates a growing stratified region at the top of the lower layer in which the local bulk density of the suspension decreases from ρ_B towards ρ_I. We shall show that the rate of entrainment into the upper layer and the rate of fall of the interface at the top of the sedimenting region depend greatly on the rate of growth of this stratified region and hence on the distribution of particle sizes.

A particular motivation for our investigation of the phenomena described above is provided by the occurrence of sedimentation from rivers as they flow into the sea. Under suitable conditions the freshwater outflow, laden with sand and silt, will initially underlie the sea water; our results show that the subsequent convective mixing will be controlled by the settling of the suspended load. Our work also finds application in describing the deposition of crystals within layered, convecting magma chambers. In both these particular cases and virtually all geophysical applications the suspended particles vary greatly in both shape and size and therefore in settling velocity. It thus seemed to us appropriate to perform experiments with particles that were non-spherical and had a fairly wide distribution in size. This immediately distinguishes our work from the many studies that employ monodisperse spherical particles. From our results, we are able to show that the differential sedimentation of particles of different sizes plays a major role in determining the evolution of many natural systems. This conclusion is a clear consequence of the theoretical description below and is discussed further in the final section. Our approach to this result is as follows.

In §2, we describe our initial laboratory experiments which provide observations of sediment-driven convection in such a two-layered system. The two layers are separated by a sharp interface which descends at a constant velocity. These observations are consistent with the theoretical description of this system that we develop in §3. The description embodies existing theories for the differential sedimentation of polydisperse suspensions and uses buoyancy arguments to bound the extent of entrainment of particles into the upper layer. The range of interfacial velocities predicted by these bounds is compared favourably in §4 with our experimental measurements for a number of particle-size distributions. Our findings are summarized and discussed in §5.

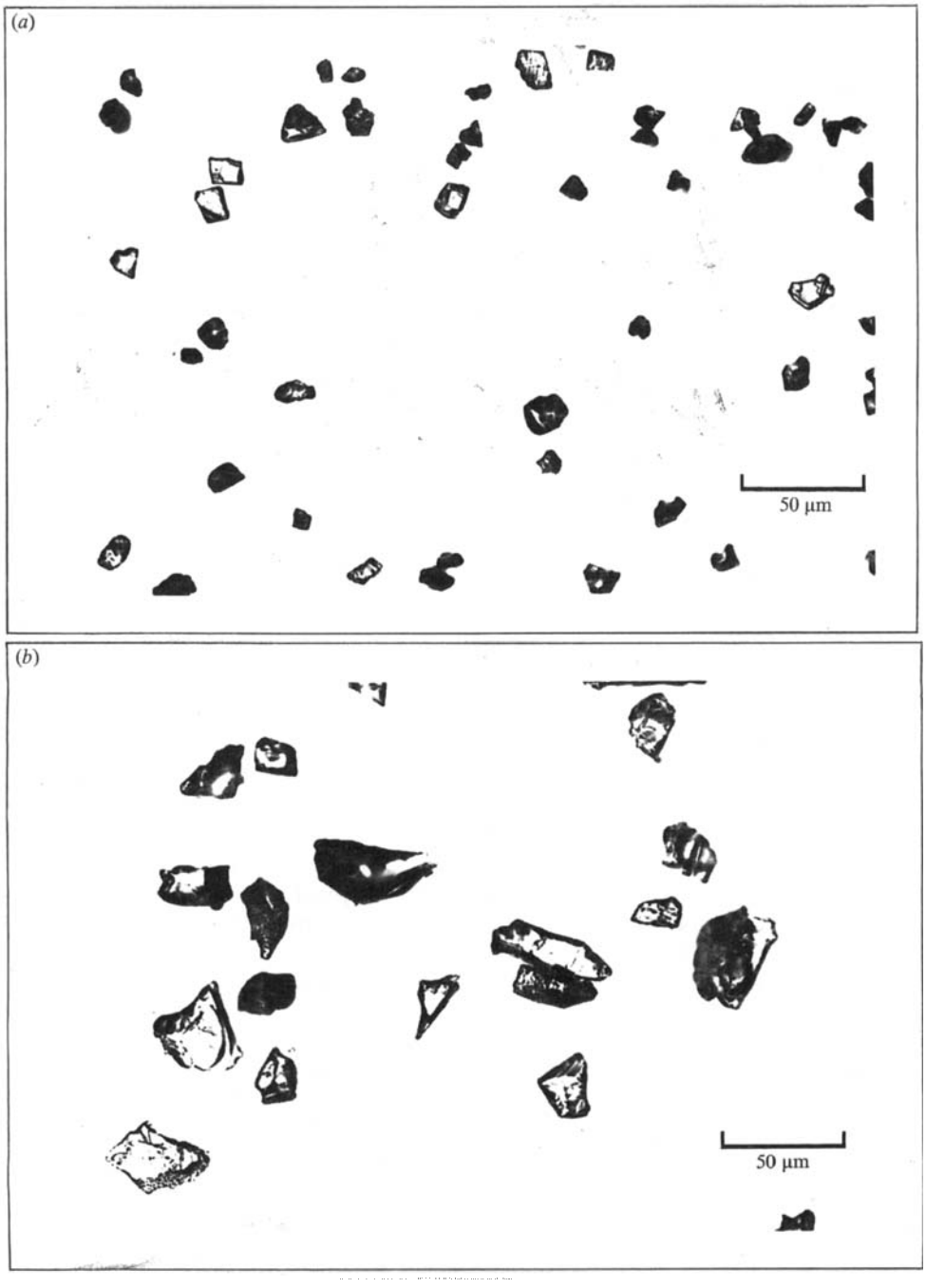

FIGURE 1. Photographs of the carborundum particles used in our experiments: (*a*) type 1 (of finer grade); (*b*) type 2 (of coarser grade).

2. Experiments

In order to conduct laboratory experiments with particles that settled out at low Reynolds number in a fluid that was sufficiently inviscid for the overlying convection to be vigorous, we needed readily available, small, dense particles. Monodisperse

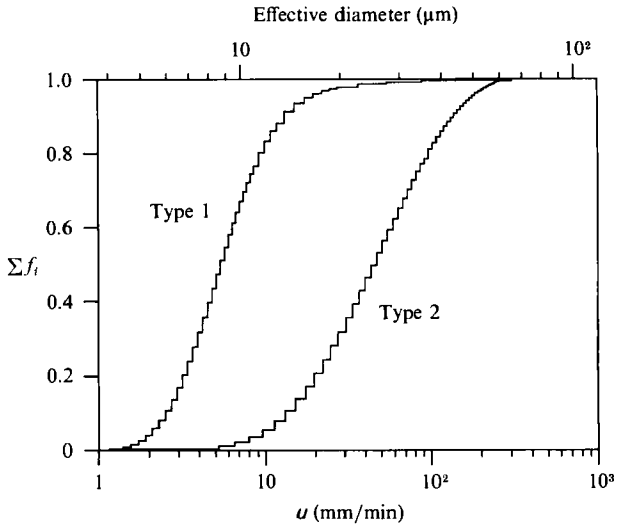

FIGURE 2. The cumulative distributions (by volume) of the settling velocity u of the particles in water. The distributions are shown discretized since both the original sedigraph measurements and the numerical results described later are based on discrete particle sizes. The discrete distribution is an approximation to the true continuous distribution as discussed in the Appendix. Also indicated are the effective diameters of spherical particles corresponding to these settling velocities.

particles that are sufficiently small for the laboratory experiments we had in mind are prohibitively expensive for the quantity we would have needed. In addition, our theoretical description shows that the effects under investigation are accentuated by polydispersion. Accordingly, after considerable searching we decided that suitable particles would be provided by two grades of commercially available carborundum (silicon carbide) grinding powders. The particles had a common density $\rho_P = 3.218$ g cm^{-3} and were irregular in shape with a typical aspect ratio of about two. Photographs of a sample of each grade are shown in figure 1. The distributions of the settling velocities of the particles in water were determined by the sedigraph technique (Jones, McCave & Patel 1988) and are shown in figure 2. From these velocity distributions and the known density of the particles we can evaluate the size distribution of the particles. The particles of type 1 (technical grade C600) had an effective median diameter of 8.7 μm, while those of type 2 (technical grade C400) had an effective median diameter of 25.0 μm, where the effective diameter is the diameter of the spherical particle that would have the same settling velocity in water at 20 °C. We chose water as the interstitial fluid to suspend the particles in the lower layer, and all fluids and particles used in the experiments were at room temperature ($\approx$ 20 °C). Early trial experiments used aqueous salt solutions for the upper layer, but led to unrepeatable results. The explanation may be that in an ionic solution the surface charges on each particle are screened by the surrounding ions, which allows the particles to approach each other closely enough for coagulation to occur (Jeffery & Acrivos 1976; Hunter 1987). In the subsequent experiments reported here the salt solutions were thus replaced by aqueous solutions of sugar (sucrose), which seemed to eliminate the problems.

The majority of the experiments were conducted in a Perspex tank which consisted of a lower region, 19.5 cm × 3 cm in cross-section and 20 cm in depth, joined at its top into the base of a much larger region, 19.5 cm × 40 cm in cross-section and 30 cm in

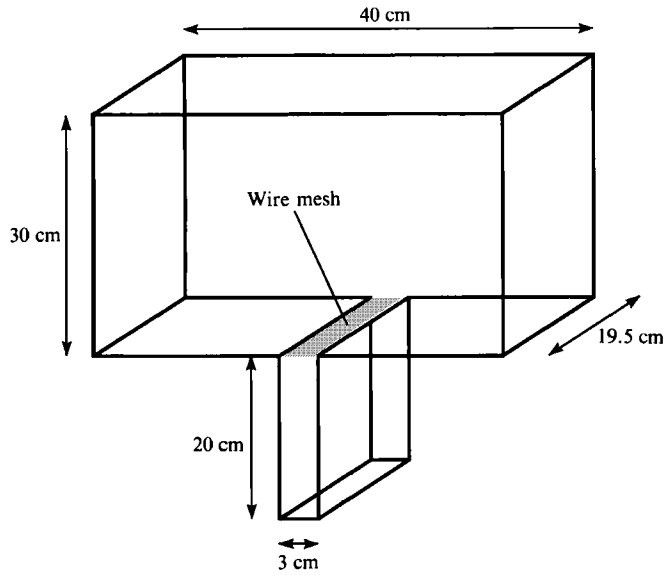

FIGURE 3. The Perspex tank used for the majority of our experiments.

depth (figure 3). The purpose of this larger region was to provide an upper fluid layer of such a large volume that its properties (and, in particular, its density) did not change significantly during the course of an experiment. A wire mesh with 2 mm openings was used to help shield the convection in the lower region from large-scale circulation in the upper region. It was observed that the mesh did not have a significant effect on the smaller-scale convection driven by the breaking away of buoyant fluid from the top of the sedimenting region.

Two different experimental procedures were used to set up the initial configuration. In many of the experiments the tank was first filled with the sugar solution. The dense suspension was then added under the sugar solution using a pipe leading from a continuously stirred reservoir to the bottom of the tank. This procedure, which typically produced a lower layer of 10 cm depth in a time of a half to one minute, resulted in negligible mixing between the fluids provided that the volume concentration of the stabilizing suspended particles was greater than approximately 1%. The remaining experiments, in particular those with lower concentrations of suspended particles, used a different filling procedure in which the entire lower region was first rapidly filled with the stirred suspension. A metal plate was then placed over the opening between the two regions and the upper region of the tank was filled with the sugar solution. Finally, the plate was gently displaced laterally and replaced by the wire mesh. This procedure took about half a minute.

Direct observations of the experiments were supplemented by both photographs and a movie. A photograph taken shortly after the start of a typical experiment is shown in figure 4. It may be seen that the settling of the particles left behind buoyant interstitial fluid. This fluid rose in thin streamers and sheets, while still carrying some suspended particles, into the overlying sugar solution where it drove vigorous convection; the convection extended through the entire depth of the overlying fluid and the lifted particles were well mixed to near the top of the tank. Detailed examination using a microscope revealed that a very sharp interface separated the convecting region from an underlying sedimenting region. Just below the interface

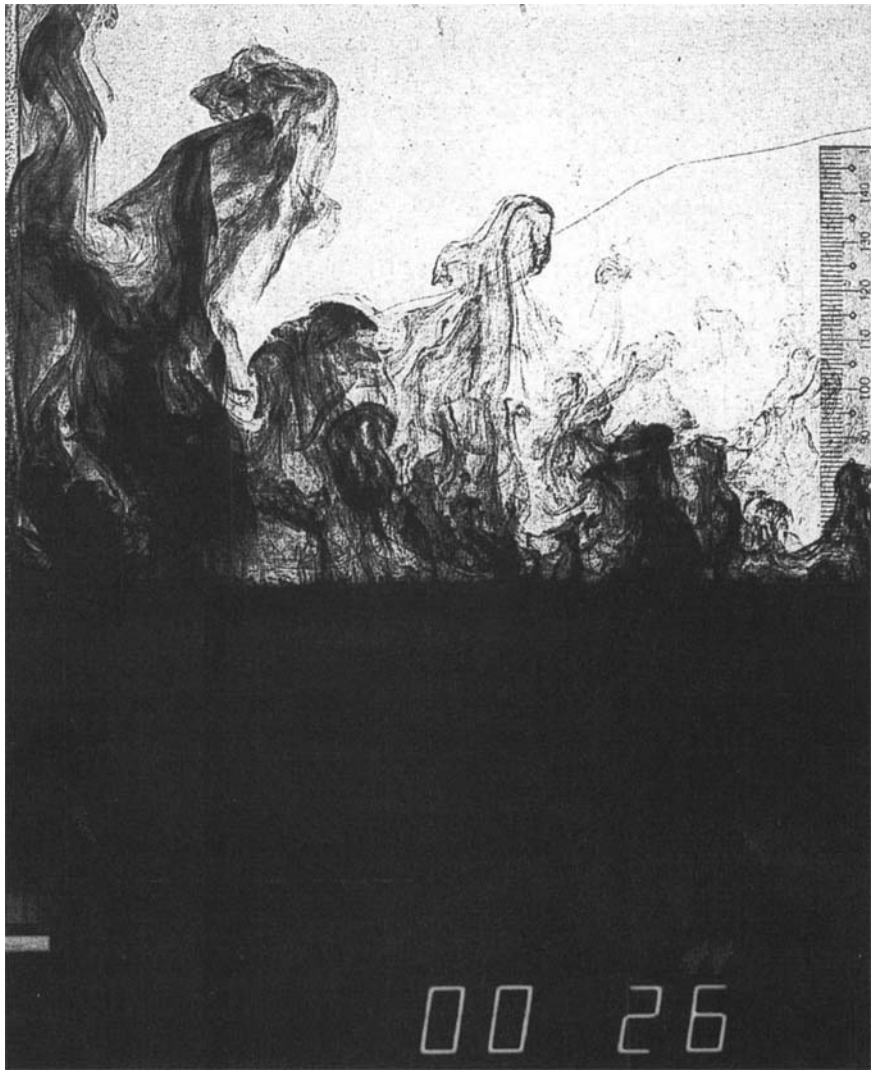

FIGURE 4. Convection in an aqueous sugar solution driven by sedimentation in an underlying suspension of carborundum grit in water. Notice the sharp interface between the two layers at approximately 60 mm from the base of the tank and also the sediment that is entrained into the upper layer. The photograph was taken 26 s after the initiation of the experiment.

wave-like motions were observed, driven by the convective motions above the interface. Further below the interface, no such motions were observed and the particles fell vertically.

These qualitative observations are consistent with three further observations made during the course of some preliminary experiments conducted in a smaller Perspex tank 15 cm × 5 cm in cross-section and 25 cm in depth. First, measurements of the refractive index of the interstitial fluid in samples drawn from the lower layer showed no detectable difference from fresh water; it follows that sugar was not transported down into the lower layer. Secondly, a number of samples were withdrawn by syringe at a given height in the sedimenting region. Measurements of the total weight of each sample and of the sediment content alone revealed that the

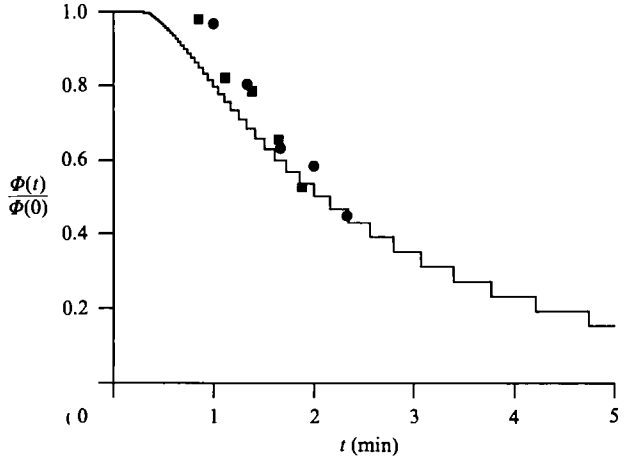

FIGURE 5. The variation with time of the volume fraction $\Phi(t)$ (normalized by its initial value $\Phi(0)$) of particles at a height of 2 cm above the base of the tank. The data are taken from two experiments with type-2 particles. In both experiments the initial bulk density of the lower layer $\rho_B = 1.076$ g cm^{-3}. In the first experiment (■) the density of the upper layer $\rho_U = 1.030$ g cm^{-3}, whereas in the second (●) there was no upper layer. In both experiments the particle concentration was initially constant and then decreased gradually. The theoretical prediction represented by the curve is calculated from the model described in §3 which is based on a discrete distribution of particle sizes.

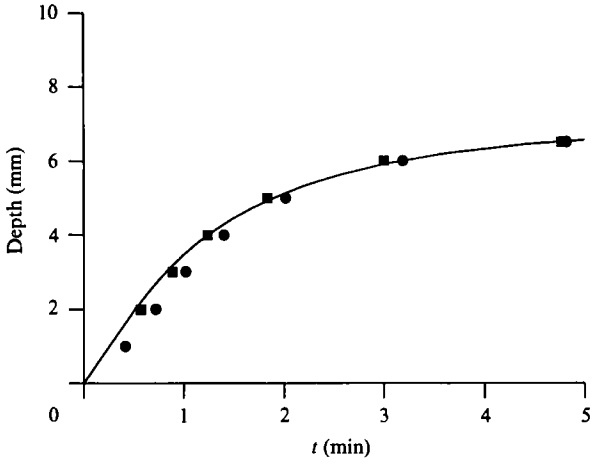

FIGURE 6. The depth of sediment accumulated at the base of the tank, in two experiments with type-2 particles. In the first experiment (■) $\rho_B = 1.076$ g cm^{-3} and $\rho_U = 1.030$ g cm^{-3}, whereas in the second (●) there was no upper layer. The measured evolution is identical after allowing for slight errors in the start times of both experiments. The rate of accumulation is seen initially to be constant and then to decrease gradually. The theoretical prediction represented by the curve is based on the model described in §3.

local concentration of particles decreased with time (figure 5). (The calculated prediction also shown in this figure will be discussed in §4 following the development of a theoretical description.) Comparison with a control experiment in which there was no upper layer, but which also exhibited a time-dependent concentration in the lower layer, showed that the rate of the decrease in the concentration was not affected by the presence or absence of a convecting upper layer. Thirdly, a

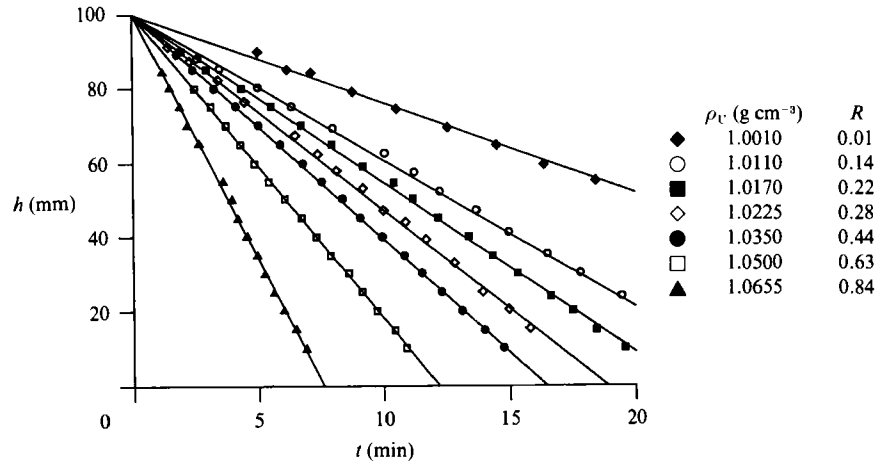

FIGURE 7. A typical set of measurements of the interfacial position from experiments which used type-1 particles, $\rho_B = 1.079$ g cm^{-3} (and therefore $\Phi = 0.0356$), and a number of values of ρ_U shown in the legend. Also shown are the corresponding values of the dimensionless ratio $R = (\rho_U - \rho_I)/(\rho_B - \rho_I)$. The origin of time in each experiment was adjusted slightly so that the best-fit lines pass through a common point. The results show both that the interfacial velocity is constant during an experiment and that it is a monotonically increasing function of R.

microscope was used to provide direct measurements of the deposition of sediment on the base of the tank. The rate of accumulation was found initially to be constant and then to decrease gradually (figure 6). This behaviour was also unaffected by the presence or absence of a convecting upper layer. The inference to be drawn from these observations is that the process of sedimentation in the lower layer is largely independent of the motion in the upper layer.

In the majority of the experiments, which were conducted in the tank shown in figure 3, the position of the interface between the upper and lower layers was monitored as a function of time until it reached the base of the tank. The measurements for a particular value of the initial bulk density of the lower layer are shown in figure 7. In each experiment the interface was observed to fall at a constant velocity V. In addition, it was apparent that, for a given distribution of the particle sizes and a given density of the lower layer, there was a systematic increase in the interfacial velocity as the density of the upper layer was increased. Both these important observations can be understood in terms of the theoretical description given below. In this description we first evaluate the fall velocity of the sediment in the lower layer. We then calculate the amount of buoyant fluid and trapped particles that is released from the top of the layer.

3. Theoretical description

Consider an initially well-mixed sediment-laden fluid region of bulk density ρ_B which consists of a volume fraction Φ of dense particles of density ρ_P and a volume fraction $1-\Phi$ of interstitial fluid of density ρ_I. The bulk density of the suspension is related to the densities of the particles and of the interstitial fluid by $\rho_B = \rho_I + \Phi(\rho_P - \rho_I)$. Let the sediment-laden region be overlain by a large volume of fluid

of density ρ_U so that, provided $\rho_B > \rho_U$, the initial bulk-density gradient is statically stable. We wish to calculate the subsequent effects of the sedimentation of the dense particles in the lower region.

In general, the suspended particles will be polydisperse with a range of settling velocities. We believe that an understanding of the fundamental concepts is most easily obtained in terms of a discrete distribution of particle sizes. Then the results for a continuous distribution may be obtained in the usual way as the limit of a large number of closely spaced particle sizes; the consequent modifications to the analysis are outlined in the Appendix. Thus we suppose that the particles have a discrete distribution of particle sizes with a proportion f_i (by volume) of particles of Stokes settling velocity u_i for $i = 1, \ldots, n$. The volume fraction of i-particles in the lower region is then initially Φf_i. We let the particles be ordered by size so that $u_1 > u_2 > \ldots > u_n$.

3.1. *Upper region of lesser density*

In order to make the case in which there is overlying convection more accessible, we first review the simpler case in which $\rho_U < \rho_I$ and there is no mixing between fluid regions. The most important effect is that large particles can sediment away from the top of the lower region more rapidly than small particles. As a result, once the sedimentation begins a number of layers form and grow at the top of the lower region; each layer contains only particles smaller than a certain size and the interfaces between the layers are defined by the vertical distances through which the different-sized particles have fallen since the beginning of sedimentation.

More specifically, as shown at a particular time in figure 8(*a*), owing to this differential sedimentation a total of n interfaces form at the top of the sedimenting region: the kth interface divides the layers out of which all the k-particles have sedimented from the layers which still contain k-particles. Thus each interface propagates downwards at a characteristic speed given by the sedimentation velocity of the 'last' particles of a certain size.

Below the first interface all the particle species are present in their original concentrations $\varphi_{i1} = \Phi f_i$. Between interface k and interface $k+1$ only particles of species $i = k+1, \ldots, n$ are present; we denote their concentrations by φ_{ik} (with $\varphi_{ik} = 0$ for $i \leqslant k$). Above the nth interface no particles are present. We denote the three layers so defined as layers 0, k and n respectively. Let the velocity of an i-particle in layer k be u_{ik} and let the total volume fraction of particles in layer k be

$$\phi_k = \sum_{i=k+1}^{n} \varphi_{ik}. \tag{3.1}$$

The velocity v_k of the kth interface is given by the velocity $u_{k,k-1}$ of the k-particles just below the interface. The volume fractions φ_{ik} may be found numerically, once the u_{ik} are specified, by solving the equations for the continuity of particle flux across each interface (Smith 1966)

$$\varphi_{ik}(v_k - u_{ik}) = \varphi_{i,k-1}(v_k - u_{i,k-1}), \quad i = k+1, \ldots, n, \tag{3.2}$$

successively for $k = 1, \ldots, n$.

The remaining problem is to find expressions for the settling velocities u_{ik} of the particles in each layer. If the suspension is very dilute then each particle falls nearly independently of the others and the settling velocity of each particle is approximately equal to its isolated Stokes settling velocity u_i. In this simple case, $v_k = u_k$, as can be shown formally from (3.2). In fact, the essence of the mechanism of layer formation described above can most readily be understood by neglecting the particle

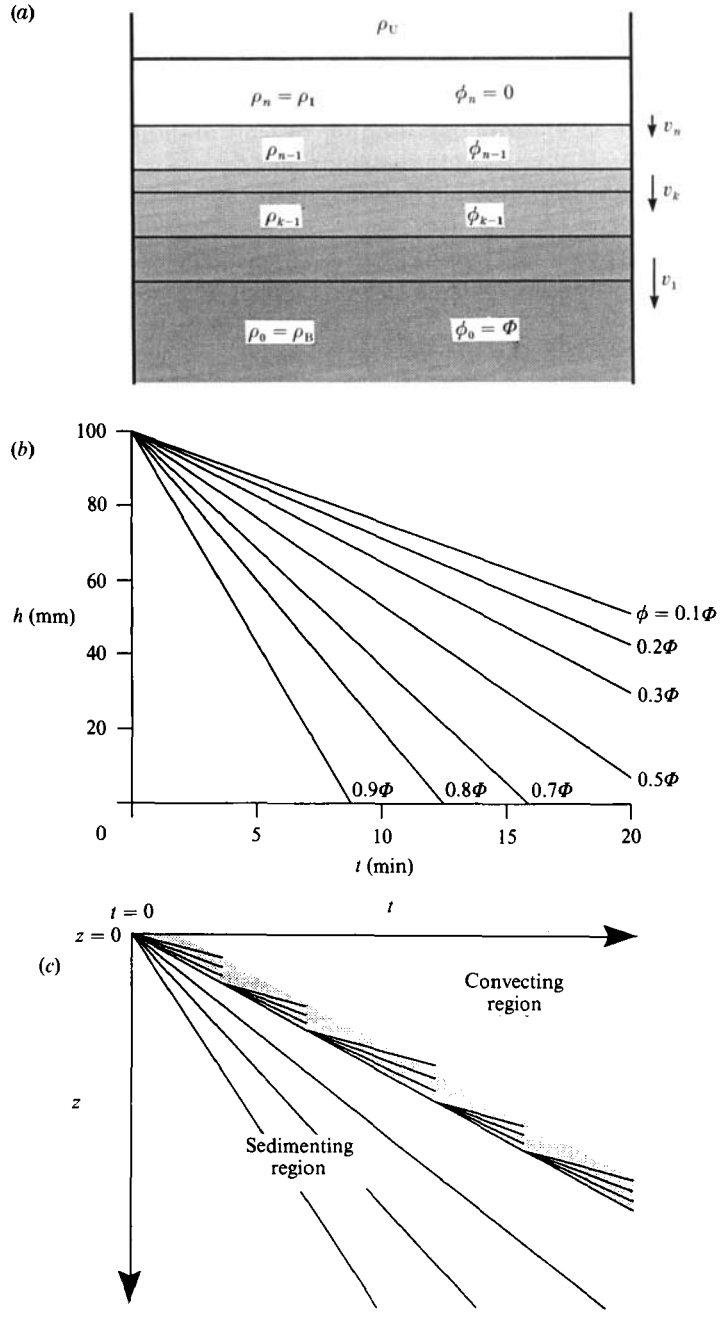

FIGURE 8. (*a*) The differential sedimentation of a suspension of particles of n discrete sizes into $n+1$ layers, each one homogeneous and with a characteristic volume fraction of particles, bulk density and settling velocity. (*b*) Calculated positions of some of the layers of constant bulk density for the differential sedimentation of a suspension of type-1 particles. The suspension initially has a uniform volume fraction $\Phi = 0.0356$ of particles, which corresponds to $\rho_B = 1.079$ g cm^{-3}, and has a total depth of 10 cm. There is no convective mixing with the overlying fluid since it is assumed that $\rho_I > \rho_U$. (*c*) A schematic representation of the successive development and convective detachment of some of the sedimenting layers for the case $\rho_I < \rho_U$. The detachment of the layers results in the descent at a constant velocity of the interface between the convecting and sedimenting regions.

interactions entirely and interpreting the interfacial velocities in figure 8(*a*) as the unhindered Stokes settling velocities.

However, for less dilute suspensions the settling of individual particles will be hindered by the presence of neighbouring particles and by the necessary upward return flow of interstitial fluid, and a formulation that includes these effects can be constructed as follows. As suggested by Greenspan & Ungarish (1982), it is convenient mathematically to write the hindering effects in the form

$$u_{ik} = U_k + \frac{F_{ik}\, u_i}{1-\phi_k}, \tag{3.3}$$

where U_k is the mean fluid velocity in the kth layer and the F_{ik} are hindered-settling coefficients which depend on all the φ_{ik}. (In ignoring the possibility of dependence on spatial gradients of the φ_{ik}, we have neglected both Brownian diffusion, because our particles are large, and self-induced hydrodynamic diffusion (Davis & Hassen 1988), which is only significant for the settling at early times of suspensions of small dispersivity.) The velocity of the return flow U_k can be eliminated between (3.3) and the equation of continuity to obtain

$$u_{ik} = \frac{F_{ik}\, u_i - \sum_{j=k+1}^{n} \varphi_{jk} F_{jk}\, u_j}{1-\phi_k}, \tag{3.4}$$

showing that the u_{ik} are coupled through their effect on the return flow. The functions F_{ik} have been evaluated to first order in ϕ_k by Batchelor (1982) and Batchelor & Wen (1982), but are unknown for general ϕ_k. For the purpose of the present calculations, therefore, we make two simplifying assumptions: first, that the F_{ik} depend only on the local total volume fraction of particles through a single hindered-settling function $\mathscr{F}(\phi_k)$ and not on the individual φ_{ik}; secondly, that the form of the hindered-settling function is adequately represented by the empirical fit

$$F_{ik} = \mathscr{F}(\phi_k) = (1-\phi_k)^5 \tag{3.5}$$

suggested by Davis & Birdsell (1988). Combining (3.4) and (3.5) gives

$$u_{ik} = (1-\phi_k)^4 \left(u_i - \sum_{j=k+1}^{n} \varphi_{jk}\, u_j \right). \tag{3.6}$$

In summary, the coupled equations (3.2) and (3.6) may be solved numerically to give the size distribution and total concentration of particles within each layer and the velocities of the interfaces between the layers. From the total concentration of particles the bulk density of each layer is readily calculated as $\rho_k = \rho_I + \phi_k(\rho_P - \rho_I)$; the densities of the layers decrease from ρ_B in the lowest layer to ρ_I in the uppermost layer as successively smaller particles fall out of the suspension. Thus we have a complete description of the sedimenting region for the case in which there is no convective mixing.

As an example, we show in figure 8(*b*) calculated solutions of (3.2) and (3.6) for a suspension of type-1 particles with $\Phi = 0.0356$. For simplicity, only some of the layers of constant density are shown.

3.2. *Upper region of greater density*

Now consider the case in which $\rho_B > \rho_U > \rho_I$. Although the initial sedimentation will still yield the sedimenting layers shown in figure 8(*a*), some of the uppermost layers will now be less dense than the overlying fluid. As the interfaces between the layers

propagate downwards, the vertical scale of these buoyant layers will grow linearly with time. When a local Rayleigh number based on the unstable stratification is sufficiently large the buoyant layers will become unstable, detach and mix convectively with the overlying fluid. This phenomenon can be likened to the detachment of a growing thermal boundary layer from a heated horizontal boundary (Lick 1965; Howard 1966). In the case considered here, during the detachment of the buoyant layers a number of the (negatively buoyant) underlying layers may also be entrained, by viscous or inertial coupling, and carried upwards. The detached material will have a negligible effect on the density of the upper region provided that the volume of that region is very large.

If the fluid viscosities are sufficiently small then, by analogy with thermal convection at large Rayleigh number, we envisage a cycle of repeated detachments as illustrated schematically in figure 8(*c*). After a certain number of layers detach from the sedimenting region, these layers will redevelop at the top of the sedimenting region; moreover, from the results of §3.1 their densities and rates of fall will be exactly the same as in the previous cycle. The density of the upper region will also be virtually unchanged since the volume of the upper region is large. Since the detachment of buoyant material must depend on the density structure in the neighbourhood of the interface between the upper and lower regions and this structure is the same from cycle to cycle, we deduce that exactly the same layers will detach in each cycle. It follows that the interface between the convecting and the sedimenting regions will fall at a constant velocity V.

It should be noted that this description of the interaction between the convecting and sedimenting regions is consistent with a number of experimental observations. Particles which fall faster than V play no role in the overlying convection and the layers in the interior of the sedimenting region evolve in the same way as the corresponding layers in the non-convecting case. Convection is driven by the generation of buoyancy in a boundary layer at the top of the sedimenting region. The sharpness of the experimental interface and the nearly continuous detachment of buoyant material are in accord with the thin boundary layers and short timescales of instability which are expected in convection at large Rayleigh number.

Though we have a good qualitative understanding of the mechanism that gives rise to a constant interfacial velocity V, we have not yet been able to predict the value of V quantitatively since we cannot calculate how much non-buoyant material is entrained by the convection. We can, however, place theoretical bounds on V from consideration of the net buoyancy of the material which detaches and convects into the upper region. It is convenient first to define dimensionless densities by

$$R = \frac{\rho_{\mathrm{U}} - \rho_{\mathrm{I}}}{\rho_{\mathrm{B}} - \rho_{\mathrm{I}}} \tag{3.7}$$

and

$$r_k = \frac{\phi_k}{\Phi} \equiv \frac{\rho_k - \rho_{\mathrm{I}}}{\rho_{\mathrm{B}} - \rho_{\mathrm{I}}}, \tag{3.8}$$

where $\rho_k = \rho_{\mathrm{I}} + \phi_k(\rho_{\mathrm{P}} - \rho_{\mathrm{I}})$ is the bulk density of layer k. In the present case of a discrete distribution of particle sizes it is convenient to let $r(v)$ be the piecewise-constant function given by the r_k and the corresponding interfacial velocities v_k. (As shown in the Appendix, an analogous function arises naturally for a continuous distribution.) Thus, in the absence of convection, $r(v)$ is the dimensionless density at $z = vt$, where z is the distance below the initial position of the interface and t is the

time since the onset of sedimentation. It follows that $R-r$ is proportional to the local buoyancy of the suspension relative to the fluid in the upper region.

The first bound on V arises from the condition that all the layers with positive buoyancy must detach. This allows us to identify a lower bound for V as the maximum velocity of an interface such that all the overlying layers are buoyant relative to the density of the fluid in the upper region. The buoyant layers are those for which $\rho_k < \rho_U$, or in non-dimensional terms $r_k < R$. Thus the lower bound, $V_{\min}$, is given by the velocity of that interface which separates $r < R$ and $r > R$. Such a condition may be expressed mathematically as

$$V_{\min} = \max_k \{v_k : r_k < R\}. \tag{3.9}$$

Secondly, an upper bound on V is given by the condition that the net buoyancy of all the detaching layers, rather than the buoyancy of each individual layer, must be positive. This condition on the net buoyancy provides an upper limit to the amount of entrainment of negatively buoyant material that can be effected by the detaching layers that have positive buoyancy. This upper limit includes any scouring of particle-laden fluid by convective motions in the upper region since it is clear that the convection itself can only be sustained if there is a net positive release of buoyancy at the base of the region. The total amount of entrainment, therefore, must be less than the value that gives rise to zero net release of buoyancy and we obtain the upper bound, $V_{\max}$, on V given by

$$\int_0^{V_{\max}} [R-r(v)]\,\mathrm{d}v = 0, \tag{3.10}$$

where an integral is used rather than a sum in order to include the possibility that $v_k < V_{\max} < v_{k+1}$ for some k, this possibility corresponding to entrainment of part of a layer.

The bounds $V_{\min}$ and $V_{\max}$ correspond to no entrainment and to maximum entrainment of negatively buoyant material respectively. Both the functions $V_{\min}(R)$ and $V_{\max}(R)$ are monotonically increasing functions of R and therefore we reasonably expect that the interfacial velocity $V(R)$, which is constrained by

$$V_{\min}(R) \leqslant V(R) \leqslant V_{\max}(R), \tag{3.11}$$

will also increase monotonically with R; and this indeed appears to be the case.

An important consequence of the detachment of the buoyant and entrained layers from the sedimenting region and the subsequent convective mixing with the overlying fluid is that some of the suspended particles are carried into the upper layer. The fraction (by volume) X of the initial suspended particle load of the lower layer that is subsequently lifted and mixed into the overlying fluid may be expressed in terms of V and the concentration of the particles in the detaching layers. The portion $X\Phi$ of the initial suspended volume fraction that gets lifted is equal to the average volume fraction of particles in the detaching layers, which are defined by $0 < v < V$. We recall that $r\Phi$ is the local volume fraction of suspended particles in order to express this average as an integral with respect to v and thereby obtain the expression

$$X = \frac{1}{V}\int_0^V r(v)\,\mathrm{d}v, \tag{3.12a}$$

after cancelling the common factor Φ on each side. Equation (3.10) may be rearranged in a form identical to that of (3.12*a*), which shows that the functional relationship between X and V is the same as that between R and $V_{\max}$. It follows that (3.12*a*) may neatly be rewritten to obtain the alternative expression

$$X = V_{\max}^{-1}[V(R)], \tag{3.12b}$$

where $V_{\max}^{-1}$ is the inverse function of $V_{\max}$. Equations (3.12) may then be used with (3.9) and (3.10) to place bounds on X. If $V = V_{\min}$ we obtain from (3.9) and (3.12*a*) the lower bound

$$X_{\min} = \sum_{k:\, r_k < R} r_k(v_k - v_{k+1})/V_{\min}, \tag{3.13}$$

where the sum is taken over the values of k that correspond to buoyant layers ($r_k < R$). In the case $V = V_{\max}$ it is clear from (3.12*b*) that the lifted fraction is given by the upper bound

$$X_{\max} = R. \tag{3.14}$$

In the simple case of a monodisperse distribution there are only two layers: layer 0 with density ρ_{B} and volume fraction Φ and layer 1 with density ρ_{I} and volume fraction zero. Thus $v_1 = u_1 \mathscr{F}(\Phi)$ and (3.11) becomes

$$v_1 \leqslant V \leqslant \frac{v_1}{1-R}. \tag{3.15}$$

The lower bound for V corresponds to the detachment of only the buoyant clear layer of density ρ_{I} and no entrainment of underlying suspension; thus $X_{\min} = 0$ in this case. The upper bound corresponds to the maximum amount of entrainment of the dense suspended particles from layer 0 into the overlying convection.

In the general case, unless R is very small, V is greater than the settling velocity v_n of the smallest particles. As $R \to 1$, we find experimentally that $V \gg v_n$, which indicates an important outcome of our investigation, namely that the rate of descent of the top of the sedimenting region can be greatly enhanced by the overlying convection. The strong dependence of V on R can be attributed to the wide range of settling velocities in our experiments and the consequently very different velocities of the various constant-density layers at the top of the sedimenting region; such a spread in velocities will also be a feature of virtually all geophysical applications. In the idealized case of a monodisperse suspension, we would expect the dependence on R to be much weaker. In this case the variation of V will be due entirely to the entrainment, which will gradually increase as the buoyancy of the interstitial fluid is increased relative to the stabilizing negative buoyancy of the initial bulk suspension.

4. Comparison of theoretical description and experimental results

The theoretical description is in good agreement with both the qualitative and quantitative experimental observations. We have observed that experimentally the process of sedimentation in the lower layer is independent of the motion in the upper layer; the particle trajectories and concentrations below the interface and the rate of accumulation at the base of the tank were all unaffected by the presence or absence of an overlying convecting layer. Theory shows that the bulk density of the polydisperse suspension in the lower layer is stably stratified (inhibiting convection)

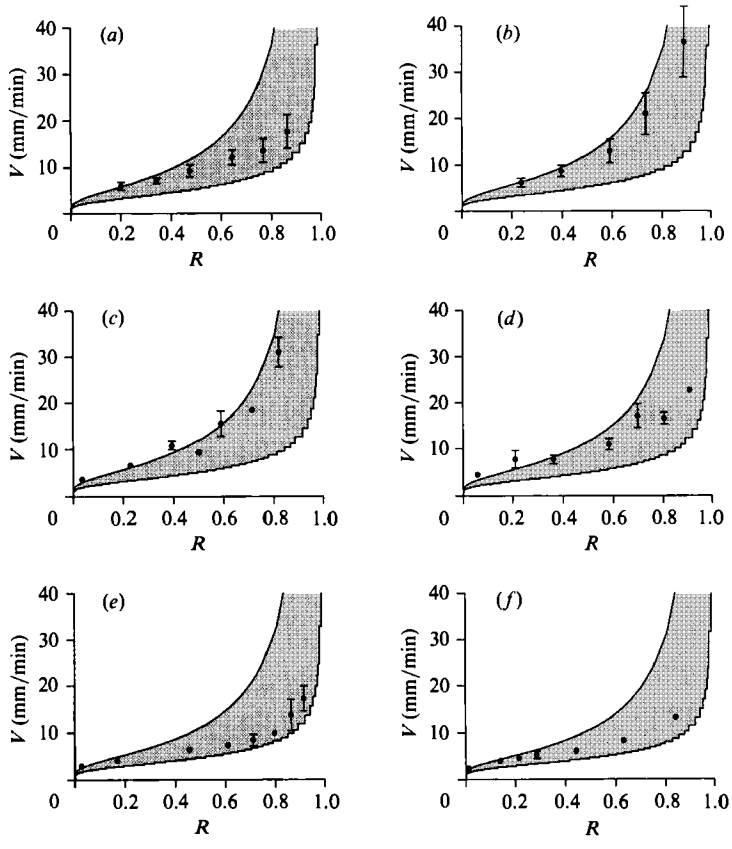

FIGURE 9. The interfacial velocities observed in experiments with type-1 particles as a function of the density ratio R for differing initial volume fractions Φ of sediment: (*a*) $\Phi = 0.0023$; (*b*) 0.0083; (*c*) 0.0126; (*d*) 0.0194; (*e*) 0.0266 and (*f*) 0.0356. Error bars, where large enough to be shown, are calculated from the statistical variation of the interfacial position with time. The curves indicate the bounding velocities, $V_{\min}(R)$ and $V_{\max}(R)$, that are predicted by (3.9) and (3.10). The step-like nature of the lower bounds results from the discrete representation of the distributions of settling velocity given in figure 2.

and suggests that convective motions are driven by a thin boundary layer at the interface and are confined to the upper layer. Hence, the motion in the lower layer consists simply of the differential sedimentation and the return flow of the interstitial fluid, in agreement with observation. This description also accounts for the decrease in the concentration of particles at a fixed point, for the decrease in the rate of accumulation at the base of the tank and for the constant velocity of the interface. From (3.2) and (3.6) the concentration of particles at a point and the rate of accumulation of sediment at the base of the tank may readily be calculated. The theoretical predictions, shown in figures 5 and 6, are in reasonable agreement with experimental measurements. The less satisfactory agreement at early times is probably due to the sedimentation being somewhat disrupted until the large-scale residual eddies generated during the input of the lower layer had died away.

A series of experimental measurements of the interfacial velocity V for a suspension of type-1 particles are presented in figure 9(*a–f*) which indicates the dependence on R for six different values of Φ. Also shown are the corresponding curves for $V_{\min}$ and $V_{\max}$ predicted from our theoretical description. We note that the experimental

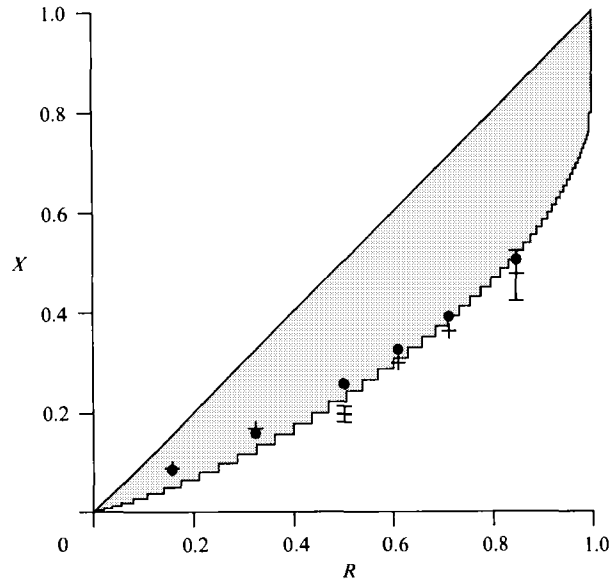

FIGURE 10. Measurements (●) of the fraction X of lifted particles in the experiments with type-2 particles and $\Phi = 0.0071$. Also shown are the values (+) calculated from the observed velocity (with error bars) using (3.12) and curves giving the bounds, $X_{\min}$ and $X_{\max}$, predicted by the theoretical model.

dependence on R is in good qualitative agreement with the predicted trend; this trend is due primarily to the polydispersivity of the particles. We note the satisfactory result that all the experimental observations are bounded below by $V_{\min}$. The comparison with $V_{\max}$ is less satisfactory, however, with some of the observations from the experiments with the intermediate values of Φ or small values of R lying a little above our computed theoretical maximum velocity.† However, neither the variation of V relative to the appropriate values of the theoretical bounds, nor the variation of V with Φ for a fixed value of R, is explained by our theoretical description, but we plan to tackle this problem in future investigations.

In a series of experiments with type-2 particles the residual fluid was decanted immediately after the end of an experiment and before the lifted particles had time to settle. The decanted particles and those that had already settled were then weighed separately, thus allowing the fraction of particles which had been lifted to be evaluated. The experimental observations, shown in figure 10 for $\Phi = 0.0071$, lie close to the theoretical minimum and agree well with the values predicted from the interfacial velocity using (3.12). In this series of experiments some of the observed values of V were slightly less than $V_{\min}$ (though by no more than experimental uncertainties). The consistency between the measurements of V and X and (3.12), however, supports the description given in §3.

Further strong support for the theoretical description is provided by the results presented in figure 11, which show the dramatic effect of varying the distribution of

† In order to test whether this discrepancy was due to premature sedimentation in the lower layer during the filling procedure, a few experiments were conducted in which the metal plate separating the upper and lower layers was not replaced by the wire mesh until five minutes after filling. When the plate was eventually displaced there was a rapid overturn of the accumulated underlying buoyant fluid. However, the interface subsequently fell at the same velocity as in experiments with undelayed starts and so this explanation must be discarded.

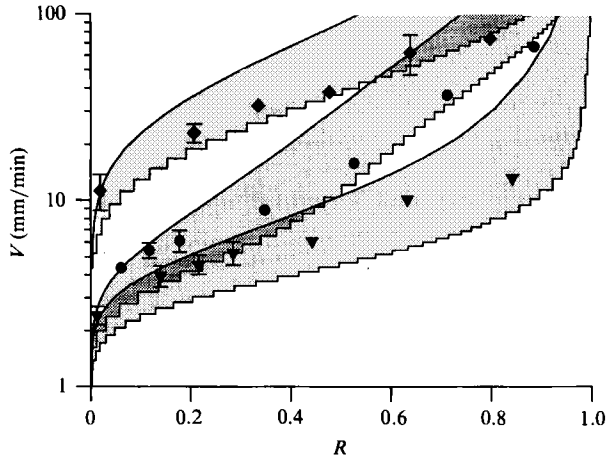

FIGURE 11. Measurements of the interfacial velocity in experiments that used a volume fraction $\Phi = 0.0356$ of type-1 particles (▾), of type-2 particles (◆) or of a mixture of equal quantities of both types of particle (●). Also shown are the corresponding maximum and minimum velocities predicted for each distribution by our theoretical model.

settling velocities and the consequent effects of polydispersion. These results are taken from three series of experiments, all with $\Phi = 0.0356$, which used, respectively, type-1 particles, type-2 particles and an equal mixture of both types. Also shown in figure 11 are the corresponding theoretical bounds (with the allowed range of velocities for each distribution stippled), which successfully bracket nearly all the observations. The similar qualitative and quantitative behaviour of the theoretical and experimental results indicates that the theoretical description accurately accounts for the effect of polydispersion on the interfacial velocity. In particular, we note that, as predicted, the observed interfacial velocities for the mixed distribution are dominated by the slowly settling type-1 component for small values of R and by the rapidly settling type-2 component for large values of R.

Though many of the experimental observations are well explained by the theoretical description, it remains to explain why a few of the observed interfacial velocities lie outside the range $V_{\min} \leqslant V \leqslant V_{\max}$ and why there is substantial variation within that range. A number of sources of error can be envisaged, which include measurement errors of the sedigraph and uncertainties in the chosen form of the hindered-settling function $\mathscr{F}$ in (3.5). We note also that the settling velocity of particles of aspect ratio 2 varies by up to 15% with orientation (Happel & Brenner 1986) and so it is necessary to assume that the average orientation of the particles in the sedigraph is similar to that in the experiments. In total, these errors might amount to about 15% in our determination of V.

In summary, the errors in the prediction of the settling distribution of the particles and some intrinsic variability between experiments (see, for example, the scatter in figures 9*c* and 9*d*) can account for the anomalous observations. Future experiments, which are planned, will attempt to reduce these sources of error.

5. Conclusions

In this paper we have analysed the novel situation in which the settling of dense sediment controls the fluid motion and evolution of a simple two-layered system. Clear fluid of density ρ_U will initially overlie a suspension in which the interstitial

fluid is less dense provided that the sediment load is sufficiently large for the bulk density of the suspension to be greater than ρ_U. As the particles sediment from the suspension, buoyant interstitial fluid is released at the base of the upper layer and drives convection in the overlying fluid. Meanwhile, differential sedimentation establishes a stable density gradient in the lower layer and inhibits fluid motion therein. The rate of release of buoyant fluid into the upper layer and the stability of the lower layer are thus both controlled by the differential sedimentation in the lower layer.

The principal parameters that determine the rate of descent of the interface between the sedimenting and the overlying regions are $R = (\rho_U - \rho_I)/(\rho_B - \rho_I)$ and the distribution of the settling velocities of the particles. In many natural applications, such as sediment transport in river systems and pyroclastic flows from volcanic eruptions, the distribution of particle sizes spans several orders of magnitude. It follows that the rate of descent of the top of the sedimenting region will also vary greatly (depending on the value of R) and will typically be very much greater than the settling velocity of the smallest particles in the suspension. In these natural examples, therefore, the polydispersivity of the suspended particles plays a dominant role in determining the rate of convective mixing of buoyant fluid into the upper layer and the volume fraction and size distribution of the lifted particles.

A theoretical description has been developed of the evolution of the lower layer, the rate of interfacial descent and the fraction of particles which are lifted. The theory provides upper and lower bounds for the interfacial velocity and for the lifted fraction. Qualitative and quantitative observations from laboratory experiments are in good agreement with the essential features of the theory, though the scatter in the current experimental data does not allow some questions to be resolved. In particular, while we can bound V and X, we cannot predict their exact values. Further experimental work is planned to address these and other issues in the many fascinating problems in which sedimentation has a controlling, dynamical influence on the bulk fluid motion.

We are grateful to Tony Beasley, Derek Corrigan and Ross Wylde-Browne for their excellent technical assistance and to David Fredericks and Gary Caitcheon of the CSIRO Division of Water Resources and Nick McCave of the Earth Sciences Department in Cambridge for the sedigraph measurements of our particles. We also acknowledge very helpful discussions with M. A. Hallworth and T. Koyaguchi, who conducted a series of similar preliminary experiments in Cambridge. An earlier draft of this manuscript was greatly improved by penetrating comments from A. Acrivos, G. K. Batchelor, R. H. Davis, H. P. Greenspan, E. J. Hinch and R. S. J. Sparks. The experimental work reported here was begun while H. E. H. spent an enjoyable period as a Visiting Fellow in the Research School of Earth Sciences, ANU, where he was supported by grants from The Royal Society and the RSES Visitors Fund. In Cambridge his work is partially supported by the BP Venture Research Unit. The manuscript was completed in Cambridge while J. S. T. was a visitor to the Institute of Theoretical Geophysics, partially supported by a grant from the NERC.

Appendix: A continuous distribution of particle sizes

For ease of understanding, we presented the discussion in the body of the paper in a form appropriate to a discrete distribution of particle sizes. We now briefly describe the case of a continuous distribution of sizes. Further details may be found in Davis,

Herbolzheimer & Acrivos (1982), Greenspan & Ungarish (1982) and Davis & Hassen (1988).

A.1. *Upper region of lesser density*

Suppose that the particles in the lower region are polydisperse, with a proportion $f_0(u)\,\mathrm{d}u$ by volume of particles with Stokes settling velocity between u and $u+\mathrm{d}u$. Thus the volume fraction of particles of differing sizes in the well-mixed lower region initially has the distribution $\varphi_0(u) = \Phi f_0(u)$. When the particles are allowed to sediment, the local distribution of the particle volume fraction $\varphi(z,t;u)$ evolves according to

$$\frac{\partial \varphi}{\partial t}+\frac{\partial(u\varphi)}{\partial z}=0, \tag{A 1}$$

for each u, where $u = u(\varphi;u)$ is the settling velocity of the particles of size represented by u in the presence of the local concentration $\varphi(z,t)$ of all other particles and z is the (downwards) distance from the initial position of the top of the sedimenting region. (It is assumed that u is a slowly varying function of z and so can be expressed as a function only of φ and u.) Since (A 1) is a form of the kinematic-wave equation, we seek solutions in which $\varphi = \varphi(v;u)$ and $u = u(v;u)$, where $v = z/t$. For such solutions, (A 1) reduces to

$$\frac{\mathrm{d}[(v-u)\varphi]}{\mathrm{d}v}=\varphi, \tag{A 2}$$

which represents the change of particle concentration $\varphi\,\mathrm{d}v$ between the planes $z = vt$ and $z = (v+\mathrm{d}v)t$ due to the difference in flux $\mathrm{d}[\varphi(u-v)]$ across them. The initial conditions are expressed by the boundary condition

$$\varphi(v;u)\to\varphi_0(u) \qquad (v\to\infty). \tag{A 3}$$

Equation (A 2) has a singular point at $v = v^*(u)$, where v^* is given by the root of $v-u(v;u) = 0$. The singular point corresponds to the trajectory of the particles of size represented by u that were initially at $z = 0$ and hence divides the region in which particles of this size are present from the region out of which all particles of this size have sedimented. Therefore, $\varphi = 0$ for $v < v^*$. It remains to specify the settling velocity u of a particle as a function of the local volume fraction occupied by all other particles. As in §3, the representation of hindered settling suggested by Greenspan & Ungarish (1982) and Davis & Birdsell (1988) may be used to obtain

$$u(v;u)=\left(1-\int_0^\infty \varphi(v;u')\,\mathrm{d}u'\right)^4\left(u-\int_0^{v^*}\varphi(v;u')\,u'\,\mathrm{d}u'\right). \tag{A 4}$$

Equations (A 2)–(A 4) are analogous to (3.2) and (3.6) and may be solved numerically. Indeed, (3.2) and (3.6) can be thought of as a particular scheme for the numerical discretization of (A 2)–(A 4) (Davis & Hassen 1988). This observation justifies our earlier decision to use a discrete formalism provided that the number of sizes of particle used to represent the distribution is sufficiently large. An alternative numerical scheme may be derived by rewriting (A 2) and (A 3) as

$$\varphi=\varphi_0\exp\left\{-\int_v^\infty \frac{\mathrm{d}u(v')}{\mathrm{d}v'}\frac{\mathrm{d}v'}{v'-u}\right\}, \tag{A 5}$$

and solving (A 4) and (A 5) iteratively for u and φ, as was done by Greenspan & Ungarish (1982).

A.2. *Upper region of greater density*

It may be observed that the cases of a discrete distribution of particle sizes and a continuous distribution of particle sizes give very similar effects during the differential sedimentation of an initially well-mixed suspension. In each case, for any given size of particle, there is a region at the top of the suspension out of which all particles of greater size have sedimented and which grows linearly with time. As a result, the bulk density near the top of the suspension decreases from ρ_B towards ρ_I and the horizontal planes of constant density each propagate downwards at a constant velocity. The only difference between the two cases is whether the density profile is continuous or stepped.

We expect, therefore, that when $\rho_I < \rho_U$ convection will be driven in the upper region for the case of a continuous distribution in a manner analogous to that described in §3 for the case of a discrete distribution: a layer of buoyant fluid at the top of the sedimenting region grows linearly with time until the local Rayleigh number exceeds a critical value and the layer detaches, together with some entrained material, and mixes with the overlying fluid. Thus the interface between the convecting and sedimenting regions will fall at a constant velocity V, which is determined by the rate of production of buoyant fluid by sedimentation and the efficiency of entrainment. As before, consideration of the buoyancy of the detaching convective boundary layer allows upper and lower bounds to be placed on V and the lifted fraction X. The lower bounds are defined by

$$r(V_{\min}) = R, \quad X_{\min} = \int_0^{V_{\min}} r(v)\,\mathrm{d}v/V_{\min}, \tag{A 6}$$

where $r(v) = \phi(v)/\Phi$, and the upper bounds are given by (3.10) and (3.14).

The critical Rayleigh number and the amount of entrainment will in detail depend on the local density profile $r(v)$ in the buoyant layer and the immediately underlying region. Therefore, a discretized representation of a continuous distribution will be a good approximation if the number of buoyant layers with $r_k < R$ is sufficiently large that $\{r_k\}$ provides a good approximation to $r(v)$ for $r < R$. Thus the approximation is least good when R is small, which may explain some of the discrepancy between theory and experiment for small R.

REFERENCES

Batchelor, G. K. 1982 Sedimentation in a dilute polydisperse system of interacting spheres. Part 1. General theory. *J. Fluid Mech.* **119**, 379–408.

Batchelor, G. K. & Wen, C.-S. 1982 Sedimentation in a dilute polydisperse system of interacting spheres. Part 2. Numerical results. *J. Fluid Mech.* **124**, 495–528.

Davis, R. H. & Acrivos, A. 1985 Sedimentation of noncolloidal particles at low Reynolds numbers. *Ann. Rev. Fluid Mech.* **17**, 91–118.

Davis, R. H. & Birdsell, K. H. 1988 Hindered settling of semi-dilute monodisperse and polydisperse suspensions. *AIChE J.* **34**, 123–129.

Davis, R. H. & Hassen, M. A. 1988 Spreading at the interface at the top of a slightly polydisperse sedimenting suspension. *J. Fluid Mech.* **196**, 107–134.

Davis, R. H., Herbolzheimer, E. & Acrivos, A. 1982 The sedimentation of polydisperse suspensions in vessels having inclined walls. *Intl J. Multiphase Flow* **8**, 571–585.

Greenspan, H. P. & Ungarish, M. 1982 On hindered settling of particles of different sizes. *Intl J. Multiphase Flow* **8**, 587–604.

Happel, J. & Brenner, H. 1986 *Low Reynolds Number Hydrodynamics.* Nijhoff.

HOWARD, L. N. 1966 Convection at high Rayleigh number. In *Proc. 11th Intl Congr. Appl. Mech., Munich*, pp. 1109–1115. Springer.

HUNTER, R. J. 1987 *Foundations of Colloid Science*. Clarendon.

JEFFERY, D. J. & ACRIVOS, A. 1976 The rheological properties of suspensions of rigid particles. *AIChE J.* **22**, 417–431.

JONES, K. P. N., MCCAVE, I. N. & PATEL, P. D. 1988 A computer-interfaced sedigraph for modal size analysis of fine-grained sediment. *Sedimentology* **35**, 163–172.

LICK, W. 1965 The instability of a fluid layer with time-dependent heating. *J. Fluid Mech.* **21**, 565–576.

SMITH, T. N. 1966 The sedimentation of particles having a dispersion of sizes. *Trans. Inst. Chem. Engrs* **44**, 153–157.